

CHAPTER 3

Methodology

Ground shaking induced by earthquakes, if large enough, can result in huge losses of life, mainly caused by building collapse. Hence, appropriate building design methods for earthquake resistance are intensively developed. However, many buildings were constructed before the emergence of the best earthquake knowledge. In other words, the earthquake resistive building design methods are developed based on learning from past earthquakes. Especially for the moderate seismicity areas in which earthquake preparation measures are limited, and there are many buildings constructed without seismic consideration. Northern Thailand also is considered as non-seismic area and therefore many of the buildings in the area are vulnerable to structural damage as the structure has inadequate seismic code enforcement. Chiang Rai province is one of the highest earthquake risk areas consisting of Mae Chan - Chiang Saen fault and Phayao faults that can cause earthquakes of magnitude 6.0 - 6.5 on the Richter scale (Ornthammarath, 2014). The maximum peak ground acceleration area from the earthquake, every 475 year period, is approximately 0.2 g on solid rock (Shedlock *et al.*, 2000; Palasri and Ruangrassamee, 2010; Ornthammarath *et al.*, 2011).

The recent big Mae Lao earthquake with a magnitude of 6.3 occurred on May 5, 2014 and caused approximately \$28 Million in damage. The epicenter of the earthquake was about 7.4 kilometers underground in Tambon Dong-Mada south of Mae Lao District and 27 kilometers southwest of Chiang Rai Municipality, Thailand (Wiwakwin and Cosuwan, 2014). The earthquake was recorded as strong, shaking both Northern region of Thailand and neighboring Myanmar. It was the strongest earthquake ever recorded in Thailand, according to National Disaster Warning Center.

Seismically, although the country has long been considered as having low seismicity, the present historical seismicity has resulted in the city to be classified as a moderate risk zone (Lukkunaprasit, 2006). As an earthquake involves rapid shaking, there is no prior warning. It is well recognized that the best way to manage this kind of disaster is to establish adequate preparedness. With the trend of providing preparedness, there has been a number of researchers concerned with earthquake loss estimation. Yeh *et al.* (2006); Malina *et al.* (2010); Reza *et al.* (2013); Wood *et al.* (2014) developed analysis modules in order to make an early loss estimation system. Hence, the Taiwan city earthquake loss estimation was performed and also a mitigation plan was proposed based on those results. In the work of Nordenson *et al.* (2000), the earthquake loss estimation for New York City was conducted providing a better understanding of how businesses and agencies create an effective mitigation plan to reduce potential damage and losses to life from future earthquakes.

Most damage and deaths caused by earthquakes are directly or indirectly as a result of ground shaking induced building collapse. This study focuses on a spatial study of the seismic performance of buildings in Chiang Rai city to establish an earthquake scenario with a magnitude of 5.0 that can lead to corresponding seismic scenarios. While the HAZUS (2001) approach is attractive, it is tailored so intimately to the U.S. situations that is difficult to apply it to other environments and geographical regions. In this study, GIS-based software (e.g., ArcGis), using the computational scheme of HAZUS, was used in conjunction with local information, as a tool for this spatial analysis. The results of the study will enable forecasting capabilities, which would be useful in anticipating the consequences of future earthquakes, and for developing plans and strategies for reducing risk. Collapse of buildings was first estimated and then the number of death caused by the building collapse was approximated. Much research in the past has resulted in the earthquake scenarios, to encourage building rehabilitation, but it has not shown the measures needed for loss reduction. The study developed earthquake scenarios in Chiang Rai city to estimate the seismic losses and changes after upgrading some of the important buildings. The aim of this study was to make people aware and showed them the benefits of upgrading some selected important buildings for seismic loss reduction.

However, most of these building are currently operational with an economically not feasible to retrofit all buildings in the Chiang Rai Municipality at the same time. Therefore, it need for a comprehensive plan to identify critical buildings and prioritize their retrofit. The retrofit prioritization incorporates qualitative and quantitative data such as site seismic hazard, building vulnerability, and building important. Thus, fuzzy models can represent qualitative aspects of knowledge to prioritizing building important integrating with quantitative data from seismic model. Finally, was using an artificial neural network approach for identification of building risk score by learning algorithm from fuzzy results. The output of proposed method by using an artificial neural network are cheaper one also time saving, especially when data are uncertain and incomplete.

This chapter provides an overview of the methodology for earthquake risk assessment. Eight topics will be discussed in this chapter: (1) Data Preparation Process, (2) Data Collection and Storage, (3) Building Risk Assessment by RVS – Method, (4) Building Damage Estimation (5) Approximation of Number of Deaths (6) Risk Mitigation and Rehabilitation (7) Fuzzy Application in Risk Model (8) Application of Artificial Neural Network for Risk Assessment. Figure 3.1 shows the overall research design.

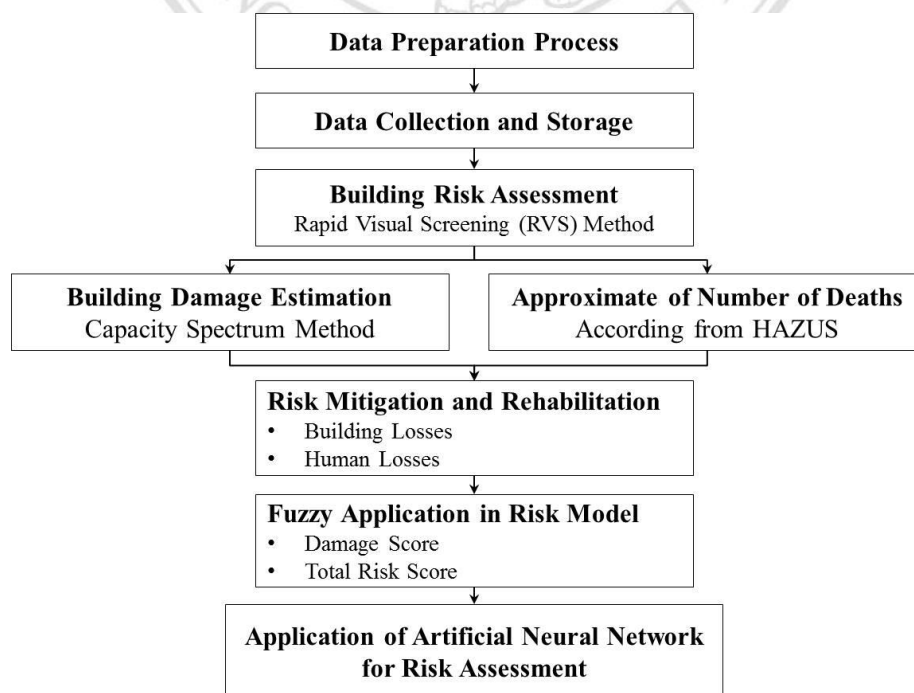


Figure 3.1 Research Methodology

3.1 Data Preparation Process

This section deals with two phases namely data preparation and process. It explains the method of collection data from site investigation. The database of sources of collecting information required for vulnerability assessment for building in the study area is also provided. To conduct this loss estimation, building data, population distribution and seismicity were spatially collected and GIS-based software was utilized in selected ward as shown in Figure 3.2.



Figure 3.2 The study area showing the 1,379 Census tracts

Figure 3.2 shows the study area in Chiang Rai Municipality. To perform the spatial analysis, the area was divided into 1,379 census tracts (size 250 x 250 m.) over the area of about 79.3 sq.km. A fieldwork plan was prepared and list of parameters were framed prior to starting actual fieldwork as follows:

- (1) Data Capture used in field survey and a data collection form based on FEMA 154.
 - Building Size
 - Number of storey
 - Building Area
 - Building occupancy
 - Building Coordinate
 - Structure Types
 - Number of persons
 - Building final score from RVS method
- (2) Data storage is transforming information from site survey to GIS system with converting the analogue data (i.e. aerial photographs, satellite images) and tabular data to digital data. The data types were entered into the GIS system as follows.
 - Spatial Data is the information about locations and shapes of geographic features and the relationships between them, usually stored as coordinates and topology.
 - Non-spatial Data is the information without inherently spatial qualities, such as associated attributes i.e. building information and final score.

3.2 Data Collection and Storage

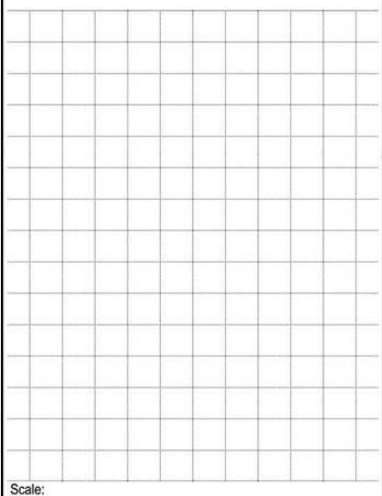
The fieldwork procedure was completed for each building through execution of the following steps:

- (1) To prepare data collection form as shown in Figure 3.3 (Moderate Seismicity Form)

- (2) Prepare a current aerial imagery and to digitize information for using in the fieldwork
- (3) To perform field survey, the aerial imagery was divided into small census tracts over the fieldwork area.
- (4) Determine the building coordinates by GPS device and fill data in the collection form.

Rapid Visual Screening of Buildings for Potential Seismic Hazards
 FEMA-154 Data Collection Form

MODERATE Seismicity

	Address: _____ _____ Zip _____ Other Identifiers _____ No. Stories _____ Year Built _____ Screener _____ Date _____ Total Floor Area (sq. ft.) _____ Building Name _____ Use _____
Scale: _____	PHOTOGRAPH

OCCUPANCY		SOIL		TYPE						FALLING HAZARDS			
Assembly	Govt	Number of Persons		A	B	C	D	E	F	<input type="checkbox"/>	<input type="checkbox"/>	<input type="checkbox"/>	<input type="checkbox"/>
Commercial	Historic	0 - 10	11 - 100	Hard	Avg.	Dense	Stiff	Soft	Poor	Unreinforced	Parapets	Cladding	Other:
Emer. Services	Industrial	101-1000	1000+	Rock	Rock	Soil	Soil	Soil	Soil	Chimneys			

BASIC SCORE, MODIFIERS, AND FINAL SCORE, S															
BUILDING TYPE	W1	W2	S1	S2	S3	S4	S5	C1	C2	C3	PC1	PC2	RM1	RM2	URM
	(MRF)	(BR)	(LM)	(RC SW)	(URM INF)	(MRF)	(SW)	(URM INF)	(TU)	(FD)	(RD)	(RD)	(RD)	(RD)	(RD)
Basic Score	5.2	4.8	3.6	3.6	3.8	3.6	3.6	3.0	3.6	3.2	3.2	3.2	3.6	3.4	3.4
Mid Rise (4 to 7 stories)	N/A	N/A	+0.4	+0.4	N/A	+0.4	+0.4	+0.2	+0.4	+0.2	N/A	+0.4	+0.4	+0.4	-0.4
High Rise (>7 stories)	N/A	N/A	+1.4	+1.4	N/A	+1.4	+0.8	+0.5	+0.8	+0.4	N/A	+0.6	N/A	+0.6	N/A
Vertical Irregularity	-3.5	-3.0	-2.0	-2.0	N/A	-2.0	-2.0	-2.0	-2.0	-2.0	N/A	-1.5	-2.0	-1.5	-1.5
Plan Irregularity	-0.5	-0.5	-0.5	-0.5	-0.5	-0.5	-0.5	-0.5	-0.5	-0.5	-0.5	-0.5	-0.5	-0.5	-0.5
Pre-Code	0.0	-0.2	-0.4	-0.4	-0.4	-0.4	-0.2	-1.0	-0.4	-1.0	-0.2	-0.4	-0.4	-0.4	-0.4
Post-Benchmark	+1.6	+1.6	+1.4	+1.4	N/A	+1.2	N/A	+1.2	+1.6	N/A	+1.8	N/A	2.0	+1.8	N/A
Soil Type C	-0.2	-0.8	-0.6	-0.8	-0.6	-0.8	-0.8	-0.6	-0.8	-0.6	-0.6	-0.6	-0.8	-0.6	-0.6
Soil Type D	-0.6	-1.2	-1.0	-1.2	-1.0	-1.2	-1.2	-1.0	-1.2	-1.0	-1.0	-1.2	-1.2	-1.2	-0.8
Soil Type E	-1.2	-1.8	-1.6	-1.6	-1.6	-1.6	-1.6	-1.6	-1.6	-1.6	-1.6	-1.6	-1.6	-1.6	-1.6

FINAL SCORE S	
COMMENTS	Detailed Evaluation Required
	YES NO

* = Estimated, subjective, or unreliable data
 DNK = Do Not Know
 BR = Braced frame
 FD = Flexible diaphragm
 LM = Light metal
 MRF = Moment-resisting frame
 RC = Reinforced concrete
 RD = Rigid diaphragm
 SW = Shear wall
 TU = Tilt up
 URM INF = Unreinforced masonry infill

Figure 3.3 Data Collection Form

- (5) Photographing the building and indicating a photo reference number in the form. In addition, Drone (Drone model Phantom 2+) was used to aerial rooftops inspection in the difficultly accessing area as shown in Figure 3.4.



Figure 3.4 Example for aerial rooftops

The aerial photography was resized and straightened by Adobe Photoshop Lightroom as shown in Figures 3.5.

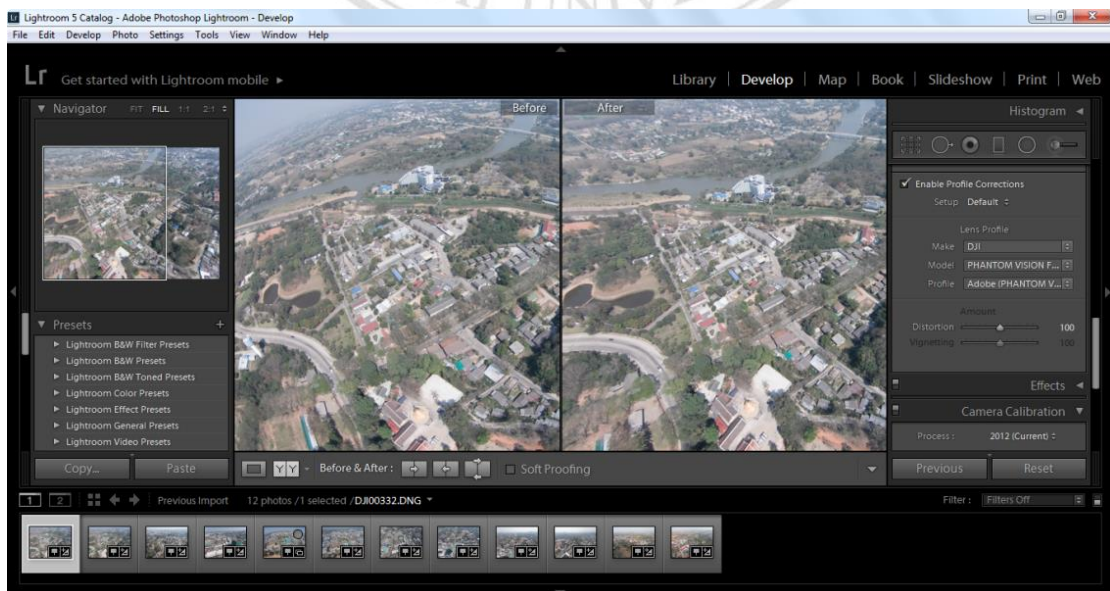


Figure 3.5 Resized and Straightened aerial photography

The data from field survey was record in GIS database through the following steps:

- (a) Check the polygon line of rooftops plan for each building and coordinate.
- (b) Define building information in the table of GIS with specified data dictionary as show in appendix A, which defines a system for associating meaning with geographic features.

3.3 Building Risk Assessment by RVS Method

Seismic evaluation of existing buildings according from FEMA (1998) have three-tiered processes (as shown in Figure 3.6) that consisting of;

- (1) Tier 1 evaluation – completion of checklists of evaluation statements that identifies potential deficiencies in a building on performance in past earthquakes.
- (2) Tier 2 evaluation – the specific evaluation of potential deficiencies to determine if they represent actual deficiencies that may require mitigation. Depending on the building type, this evaluation may be a Full-Building Tier 2 Evaluation, Deficiency – Only Tier 2 Evaluation, or a Special Procedure Tier 2 Evaluation.
- (3) Tier 3 evaluation – a comprehensive building evaluation implicitly recognizing nonlinear responses.

ลิขสิทธิ์มหาวิทยาลัยเชียงใหม่
Copyright© by Chiang Mai University
All rights reserved

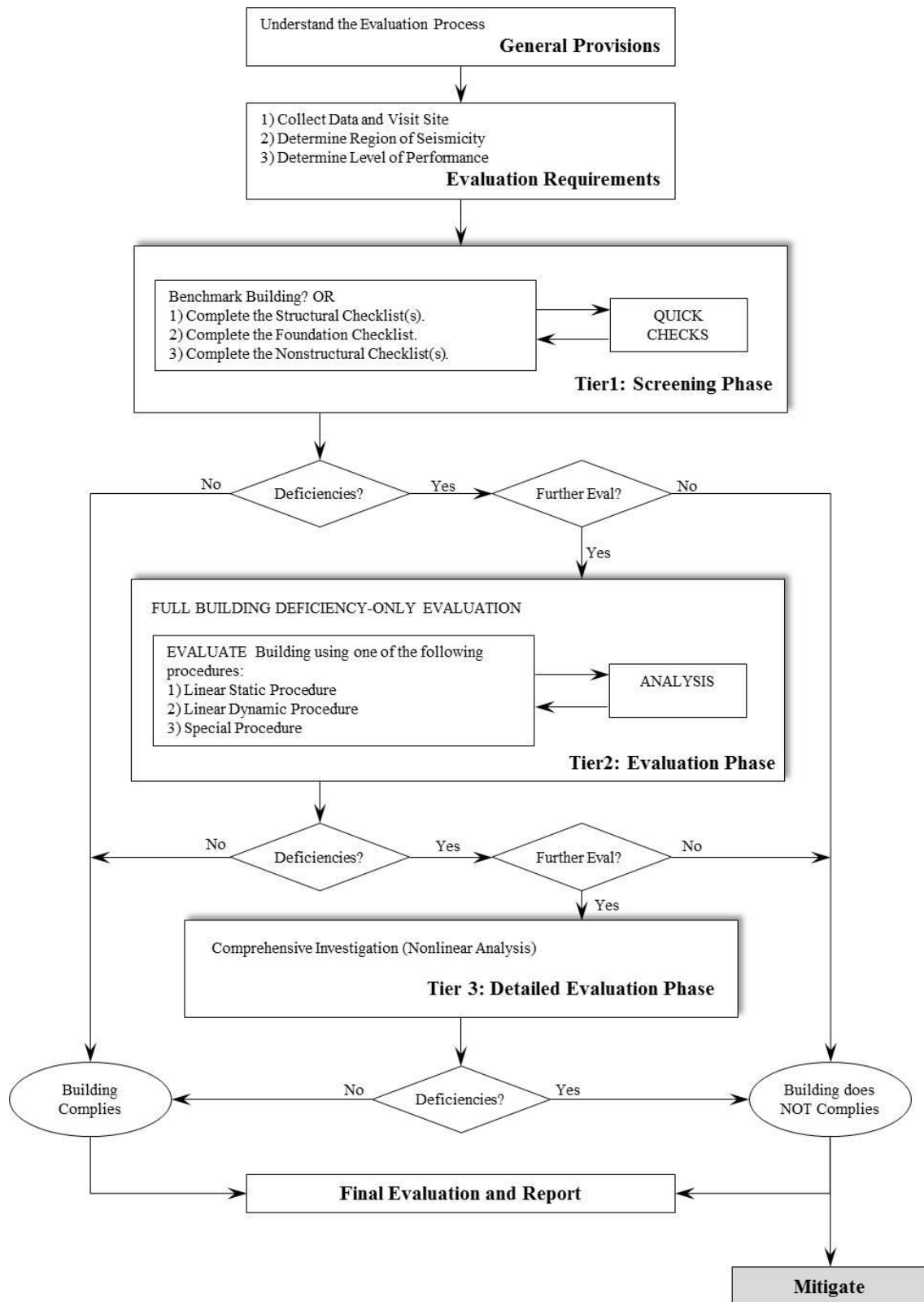


Figure 3.6 Evaluation Process (FEMA 310, 1998)

According to Figure 3.5, the evaluation process consists of screening phase (Tier 1), evaluation phase (Tier 2), and detailed evaluation phase (Tier 3). In this part the screening phase (Tier 1) consists of 3 sets of checklists that allow a rapid evaluation of the structural, nonstructural and foundation/geologic hazard elements of the building and site conditions. The screening phase is to screen and quickly identify potential deficiencies. If deficiencies are identified for a building using the checklists, the design professional may proceed to Tier 2 and conduct a more detailed evaluation of the building or conclude the evaluation and state that potential deficiencies were identified. In some cases a Tier 2 or Tier 3 evaluation may be required.

For the screening phase (Tier 1), the RVS method was used to inspect each building and classified both in term of their use, or occupancy class, and in terms of their structural system, or model building type. The methodology for calculations are based on all 28 occupancy classes and 36 model building types as shown in Tables 3.1 and 3.2 NEHRP Handbook for the seismic Evaluation of Buildings – A Prestandard (FEMA, 1998).

Table 3.1 Occupancy Class of HAZUS

No	Label	Occupancy class	Description
Residential			
1	RES1	Single family dwelling	Detached house
2	RES2	Mobile home	Mobile home
3	RES3	Multi family dwelling	Apartment/condominium
4	RES4	Temporary lodging	Hotel/motel
5	RES5	Institutional dormitory	Group housing (military, college), jails
6	RES6	Musing home	-
Commercial			
7	COM1	Retail trade	Store
8	COM2	Wholesale trade	Warehouse
9	COM3	Personal and repair service	Service station/shop
10	COM4	Professional/technical service	Office

Table 3.1 Occupancy Class of HAZUS (continued)

No	Label	Occupancy class	Description
11	COM5	Bank/financial institutions	-
12	COM6	Hospital	-
13	COM7	Medical office/clinics	Office
14	COM8	entertainment	Restaurants/bars
15	COM9	theatres	Theatres
16	COM10	Parking	Garage
Industrial			
17	IND1	heavy	Factory
18	IND2	light	Factory
19	IND3	Food/drug/chemicals	Factory
20	IND4	Metals/mineral processing	Factory
21	IND5	High technology	Factory
22	IND6	Construction	Office
Agriculture			
23	AGR	Agriculture	-
Religion/Non-Profit			
24	REL	Church	-
Government			
25	GOV1	General services	Office
26	GOV2	Emergency response	Police/fire station
Education			
27	EDU1	School/libraries	
28	EDU2	Universities/college	Does not include group housing

Table 3.2 Model building types of HAZUS

No	Label	Description	Height			
			Range		Typical	
			Name	Stories	Stories	m.
1	W1	Wood Light Frame (smaller than 464.52 sq.m.)	-	all	1	4.3
2	W2	Wood, Greater than 464.52 sq.m.	-	all	2	7.3
3	S1L	Steel Moment Frame	Low-Rise	1-3	2	7.3
4	S1M		Mid-Rise	4-7	5	18.3
5	S1H		High-Rise	8+	13	17.07
6	S2L	Steel Braced Frame	Low-Rise	1-3	2	7.3
7	S2M		Mid-Rise	4-7	5	18.3
8	S2H		High-Rise	8+	13	17.07
9	S3	Steel light Frame	-	all	1	4.6
10	S4L	Steel Frame with Cast-in-Place Concrete Shear Walls	Low-Rise	1-3	2	7.3
11	S4M		Mid-Rise	4-7	5	18.3
12	S4H		High-Rise	8+	13	17.07
13	S5L	Steel Frame with Unreinforced Masonry Infill Walls	Low-Rise	1-3	2	7.3
14	S5M		Mid-Rise	4-7	5	18.3
15	S5H		High-Rise	8+	13	17.07
16	C1L	Concrete Moment Frame	Low-Rise	1-3	2	6.10
17	C1M		Mid-Rise	4-7	5	15.24
18	C1H		High-Rise	8+	12	36.58
19	C2L	Concrete Shear Wall	Low-Rise	1-3	2	6.10
20	C2M		Mid-Rise	4-7	5	15.24
21	C2H		High-Rise	8+	12	36.58
22	C3L	Concrete Frame with Unreinforced Masonry infill Walls	Low-Rise	1-3	2	6.10
23	C3M		Mid-Rise	4-7	5	15.24
24	C3H		High-Rise	8+	12	36.58
25	PC1	Pre-Cast concrete Tilt-up Walls	-	all	1	15
26	PC2L	Pre-Cast Concrete Frame with Concrete Shear Walls	Low-Rise	1-3	2	6.10
27	PC2M		Mid-Rise	4-7	5	15.24
28	PC2H		High-Rise	8+	12	36.58
29	RM1L	Reinforced Masonry Bearing walls with Wood or Metal Deck Diaphragms	Low-Rise	1-3	2	6.10
30	RM1M		Mid-Rise	4+	5	15.24

Table 3.2 Model building types of HAZUS (continued)

No	Label	Description	Height			
			Range		Typical	
			Name	Stories	Stories	m.
31	RM2L	Reinforced Masonry Bearing walls with Wood Pre-cast Concrete Diaphragms	Low-Rise	1-3	2	6.10
32	RM2M		Mid-Rise	4-7	5	15.24
33	RM2H		High-Rise	8+	12	36.58
34	URML	Unreinforced Masonry Bearing Walls	Low-Rise	1-2	1	4.57
35	URMM		Mid-Rise	3+	3	11.89
36	MH	Mobile Homes	-	all	1	3.66

Table 3.2 describes model building type and their heights, where are used in the determination of generic-building capacity curve properties to assessing overall building performance, loss of function and casualties. The occupancy class is important to determining economic loss, since building value is closely related to the building use.

In order to arrive at final score “S” for the building under review, a series of score modification factor were assigned based on judgment such that when added/subtracted to BSH. The final score is related to probability of the building sustaining life threatening damage should a severe earthquake in the region. A building’s final score less than 2 suggests that the building is vulnerable and needs details analysis, whereas higher indicates that the building is probably adequate. The damage potential can be estimated base on the RVS score and classifications based on the European Macro-seismic Scale (EMS-98) is given in Table 3.3.

Copyright© by Chiang Mai University
All rights reserved

Table 3.3 Final Score (S) with damage potential (Grünthal, 1998)

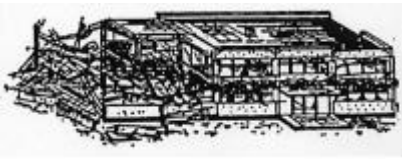
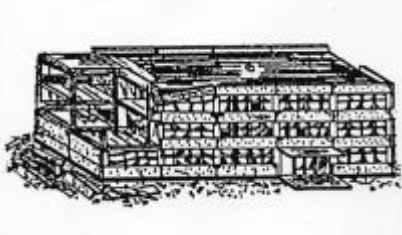
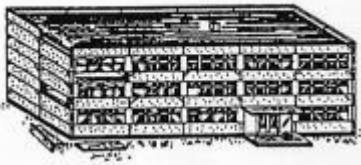
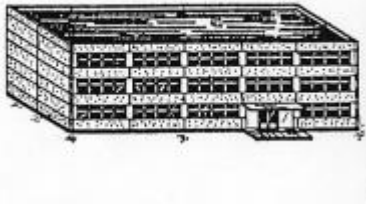
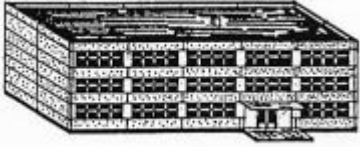
Final Score (S)	Damage Potential (EMS-98)	
S<0.3	<p>Grade 5: Destruction (very heavy structure damage)</p> <p>Collapse of ground floor parts (e.g. wings) of the building.</p>	 <p>(Grünthal, 1998)</p>
0.3<S<0.7	<p>Grade 4: Very heavy damage (Heavy structural damage, very heavy non-structural damage)</p> <p>Large cracks in structural elements with compression failure of concrete and fracture of rebars; bond failure of beam reinforcing bars; tilting of columns. Collapse of a few columns or of a single upper floor.</p>	 <p>(Grünthal, 1998)</p>
0.7<S<2.0	<p>Grade 3: Substantial to heavy damage (Moderate structural damage, heavy non-structural damage)</p> <p>Cracks in columns and beam-column joints of frames at the base and at joints of coupled walls. Spalling of concrete cover, buckling of reinforced bars. Large cracks in partition and infill walls, failure of individual infill panels.</p>	 <p>(Grünthal, 1998)</p>
2.0<S<2.5	<p>Grade 2: Moderate damage (Slight structural damage, moderate non-structural damage)</p> <p>Cracks in columns and beams of frames and in structural walls. Crack in partition and infill walls; fall of brittle cladding and plaster. Falling mortar from the joints of the wall panels.</p>	 <p>(Grünthal, 1998)</p>

Table 3.3 Final Score (S) with damage potential (continued)

Final Score (S)	Damage Potential (EMS-98)	
S>2.5	<p>Grade 1: Negligible to slight damage</p> <p>(No structural damage, slight non-structural damage)</p> <p>Fine cracks in plaster over frame members or in walls at the base</p> <p>Fine cracks in partitions and infills.</p>	 <p>(Grünthal, 1998)</p>

3.4 Building Damage Estimate

The Building damage estimation in this study was based on the concept of the Capacity-spectrum method. This method combines the ground motion input in terms of the response spectra (spectral acceleration versus spectral displacement, as shown in Figure 3.7) with the building's specific capacity curve (Figure 3.8) varying in building type, construction quality and local building regulations. The philosophy is that any building is structurally damaged by its permanent displacement (and not by the acceleration by itself). For each building type the inter-story drift is a function of the applied lateral force that can be analytically determined and transformed into building curves (capacity to withstand accelerations without permanent displacements). Using the assumption of similar structural performances, the capacity curves for 36 U.S. building types developed by FEMA (2003) were used in this study. The curves have been adopted in earthquake damage estimation in a HAZUS analysis. It is noted that structural performance of the existing buildings were assumed to complying with pre-seismic code construction regulations, as shown in Table 3.4.

Table 3.4 Capacity Curve for Pre-Code Seismic Design Level

Building Type	Yield Capacity Point		Ultimate Capacity Point	
	D_y (cm.)	A_y (g)	D_u (cm.)	A_u (g)
W1	0.61	0.200	10.97	0.600
W2	0.41	0.100	5.97	0.250
S1L	0.38	0.062	6.99	0.187
S1M	1.12	0.039	13.54	0.117
S1H	2.95	0.024	26.62	0.073
S2L	0.41	0.100	4.78	0.200
S2M	1.55	0.083	12.32	0.167
S2H	4.93	0.063	29.51	0.127
S3	0.41	0.100	4.78	0.200
S4L	0.25	0.080	3.30	0.180
S4M	0.69	0.067	6.25	0.150
S4H	2.21	0.051	14.94	0.114
S5L	0.30	0.100	3.05	0.200
S5M	0.86	0.083	5.77	0.167
S5H	2.77	0.063	13.84	0.127
C1L	0.25	0.062	4.47	0.187
C1M	0.74	0.052	8.79	0.156
C1H	1.27	0.024	11.48	0.073
C2L	0.30	0.100	4.57	0.250
C2M	0.66	0.083	6.60	0.208
C2H	1.88	0.063	14.00	0.159
C3L	0.30	0.100	3.43	0.225
C3M	0.66	0.083	4.95	0.188
C3H	1.88	0.063	10.49	0.143
PC1	0.46	0.150	5.49	0.300
PC2L	0.30	0.100	3.66	0.200
PC2M	0.66	0.083	5.28	0.167
PC2H	1.88	0.063	11.20	0.127
RM1L	0.41	0.133	4.88	0.267
RM1M	0.89	0.111	7.04	0.222
RM2L	0.41	0.133	4.88	0.267
RM2M	0.89	0.111	7.04	0.222
RM2H	2.49	0.085	14.94	0.169

Table 3.4 Capacity Curve for Pre-Code Seismic Design Level (continued)

Building Type	Yield Capacity Point		Ultimate Capacity Point	
	D_y (cm.)	A_y (g)		D_y (cm.)
URML	0.61	0.200	6.10	0.400
URMM	0.69	0.111	4.60	0.222
MH	0.46	0.150	5.49	0.300
S3C3	0.36	0.100	4.11	0.213
W1C3	0.46	0.150	7.21	0.413
W2C3	0.36	0.100	4.70	0.238

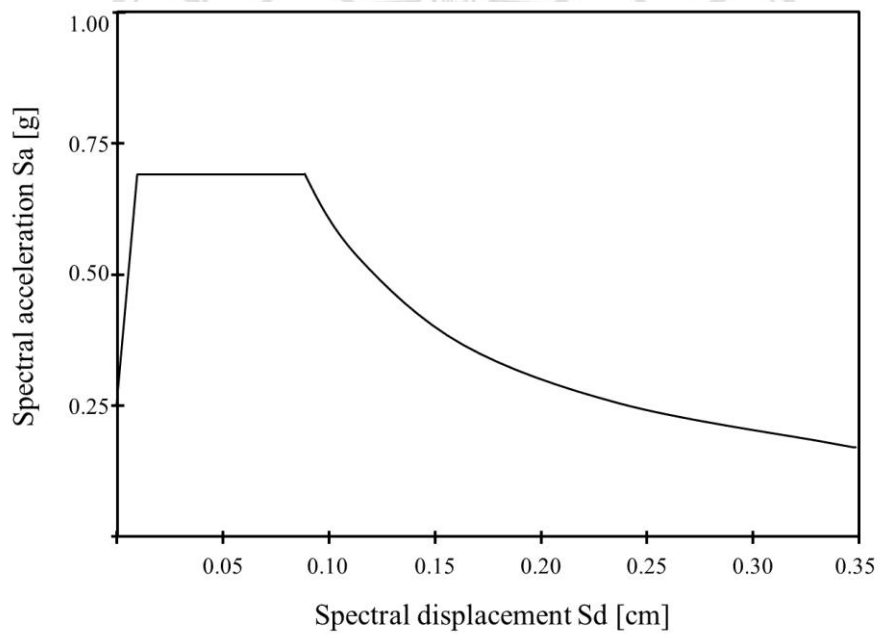


Figure 3.7 The ground-motion response spectral ordinates of spectral acceleration versus spectral displacement

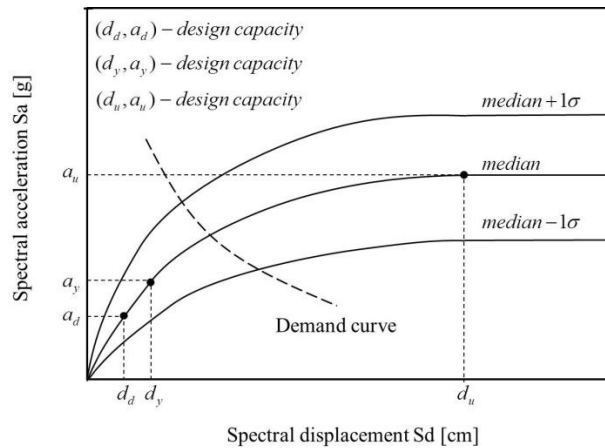


Figure 3.8 Principle of the building specific capacity curve intersected by the load curve representing the seismic demand

In Figure 3.7, the building capacity curve is defined through three control points i.e., design, yield and ultimate capacity, respectively. Up to the yield point, the building capacity curve is assumed to behave elastically linear. From the yield point to the ultimate point, the capacity curve changes from an elastic to a fully plastic state (curved form), and the curve is assumed to remain fully plastic past the ultimate point (linear form). A bi-linear representation (two linear parts) is sometimes used to simplify the model. The vulnerability curves or fragility curves are developed as log-normal probability distributions of damage from the capacity curves, as shown in Figure 3.9. The structural damage states are divided into four damage states i.e., slight, moderate extensive, and complete, respectively.

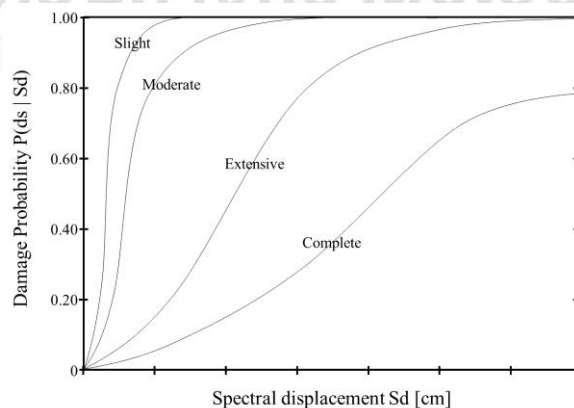


Figure 3.9 Example of fragility curve showing the probability $P(ds|Sd)$ of being in or exceeding the different damage state, d_s

A key point in any seismic risk assessment is the provision of seismic ground motion which following, spectral accelerations at the three periods $T = 0.01(s)$ peak ground acceleration (PGA), $T = 0.30(s)$ ($Sa_{0.3}$) and $T = 1.0(s)$ ($Sa_{1.0}$) have to be provided in order to describe the elastic design spectrum. As shown in Figure 3.10, the spectrum consists four parts (1) PGA , a region of constant spectral acceleration at periods from zero seconds to T_{AV} , (2) a region of constant spectral velocity between periods from T_{AV} to T_{VD} , and a region of constant spectral displacement for periods of T_{VD} . Figure 3.10 depicts the seismic design values are based on a building with an assumed 5% of critical damping, which means changes in overall stress within a structure subject to shock and vibration, with frequent arguments whether a structure will has 5% ($\xi = 5\%$) structural damping.

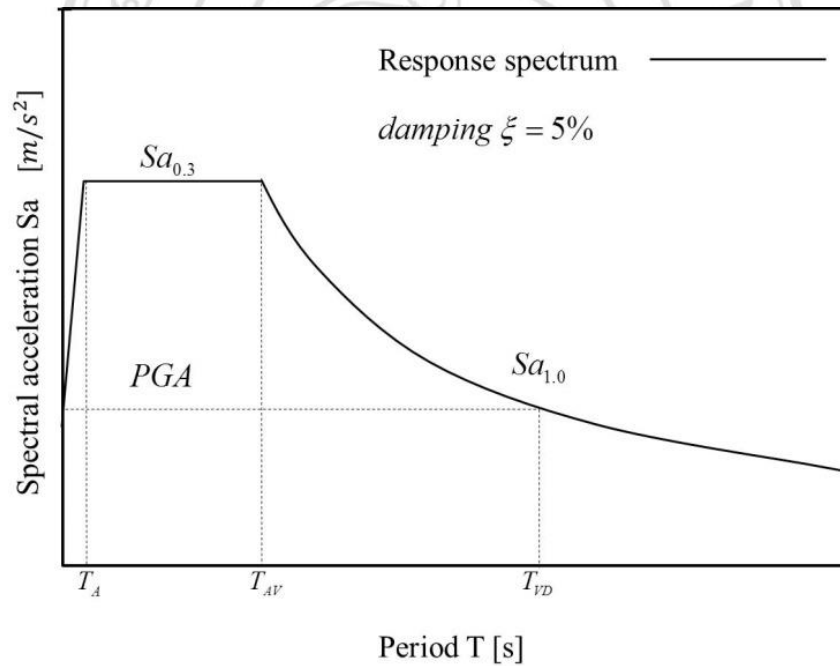


Figure 3.10 Standard shape of the response spectrum

The region of constant spectral acceleration is defined by the constant Sa at 0.3s ($Sa_{0.3}$). The region of constant spectral velocity has Sa proportional to $1/T$ and is anchored to the constant Sa at 1.0s ($Sa_{1.0}$). In general, the elastic design spectrum $Sa(T)$ is defined by the following equations

$$Sa(T) = Sa_{0.3} \times \left(0.4 + \frac{T}{T_A}\right) \quad \text{for } T < T_A \quad (3.1)$$

$$Sa(T) = Sa_{0.3} \quad \text{for } T < T < T_{AV} \quad (3.2)$$

$$Sa(T) = \frac{Sa_{1.0}}{T_A} \quad \text{for } T_{AV} < T < T_{VD} \quad (3.3)$$

$$Sa(T) = \frac{Sa_{1.0} \times T_{VD}}{T^2} \quad \text{for } T_{VD} < T < 10s \quad (3.4)$$

The period T_{AV} is based on the intersection of the region of constant spectral acceleration and constant spectral velocity. Its value varies depending on the values of spectral acceleration that define these two intersecting regions:

$$T_{AV} = \frac{Sa_{1.0}}{Sa_{0.3}} \quad (3.5)$$

The period T_A representing the left corner period of the spectral plateau can be determined as follows:

$$T_A = 0.2 \times T_{AV} = 0.2 \times \left(\frac{Sa_{1.0}}{Sa_{0.3}} \right) \quad (3.6)$$

The constant spectral displacement region has spectral acceleration proportional to $1/T^2$ and is anchored to the spectral acceleration value at the period T_{AV} , where constant spectral velocity transitions to constant spectral displacement. In order to be able to describe the elastic design spectra (for rock: site class B) in case that the *PGA* is given, the following expressions have to be regarded:

$$Sa_{0.3} = Sa_{AS} = 2.5 \times PGA \quad (3.7)$$

$$Sa_{1.0} = Sa_{AL} = PGA \quad (3.8)$$

The methodology amplifies rock (site class B) *PGA* by same factor as the specified in Table 3.5 for short period (0.3s) spectral acceleration.

Table 3.5 Site amplification factors as given in IBC-2006

Site Class B Spectral Acceleration	Site Class				
	A	B	C	D	E
Short – Period, S_{AS} [g]	Short – Period Amplification Factor, F_A				
≤ 0.25	0.8	1.0	1.2	1.6	2.5
(0.25, 0.50]	0.8	1.0	1.2	1.4	1.7
(0.50, 0.75]	0.8	1.0	1.1	1.2	1.2
(0.75, 1.0]	0.8	1.0	1.0	1.1	0.9
> 1.0	0.8	1.0	1.0	1.0	0.9
1-Second Period, S_{AL} [g]	1-Second Period Amplification Factor, F_V				
≤ 1.0	0.8	1.0	1.7	2.4	3.5
(0.1, 0.2]	0.8	1.0	1.6	2.0	3.2
(0.2, 0.3]	0.8	1.0	1.5	1.8	2.8
(0.3, 0.4]	0.8	1.0	1.4	1.6	2.4
> 0.4	0.8	1.0	1.3	1.5	2.4

$$PGA_i = PGA \times F_{Ai} \quad (3.9)$$

From the equation (3.9), PGA_i is the PGA for site class i , PGA is that for site class B and F_{Ai} is the short period amplification factor for site class i , for spectral acceleration S_{AS} . The construction of demand spectra including soil effects is done using the following equations for short periods in equation (3.10) and for long periods in equation (3.11), respectively. Then, the period T_{AVi} , which defines the transition period from constant spectral acceleration to constant spectral velocity is a function of the site class. It can be determined by the equation (3.12).

$$S_{ASi} = S_{AS} \times F_{Ai} \quad (3.10)$$

$$S_{ALi} = S_{AL} \times F_{Vi} \quad (3.11)$$

$$T_{AVi} = \frac{S_{AL} F_{Vi}}{S_{AS} F_{Ai}} \quad (3.12)$$

where:

- S_{ASi} : short-period spectral acceleration for site class i , in unit of $[g]$
- S_{AS} : short-period spectral acceleration for site class B, in unit of $[g]$
- F_{Ai} : short-period amplification factor for site class i and for spectral acceleration S_{AS}
- S_{ALi} : 1-second (long) period spectral acceleration for site class i , in unit of $[g]$
- S_{AL} : 1-second (long) period spectral acceleration for site class B, in unit of $[g]$
- F_{Vi} : short-period amplification factor for site class i and for spectral acceleration S_{AL}
- T_{AVi} : transition period between constant spectral acceleration and constant spectral velocity for site class i , in unit of $[s]$

Note that the period T_{VD} , defines the transition period from constant spectral velocity to constant spectral displacement. For the evaluation of structural damage it is more convenient to plot the acceleration response spectrum as a function of spectral displacement (rather than period). This could be achieved due to the relation between the different spectral parameters:

$$\frac{Sa}{\omega} = Sv = Sd \cdot \omega \quad (3.13)$$

where:

- ω : Circular natural frequency

The final result of this process is the computation of a 5% damped response spectrum at the center of each geographical unit (where values of ground motion were computed) or at the specific site under study.

The building response (e.g., peak displacement) is determined by the intersection of the seismic demand spectrum and the building capacity curve. The demand spectrum is based on the PESH in put spectrum reduced for effective damping (when effective damping exceeds the 5% damping level of the PESH input spectrum). The elastic response spectra provided as a PESH input applies only to buildings that remain elastic during the entire ground shaking time history and have elastic damping values equal to 5%. This is generally not true on both accounts. Therefore, elastic response spectra are modified in case of (a) buildings pushed beyond their elastic limits and thus dissipating hysteretic energy, and (b) buildings with elastic damping not equal to 5%. Modifications are represented by reduction factors through which the spectral ordinates are divided to obtain the damped demand spectra. The methodology reduces demand spectra for effective damping greater than 5% based on statistically – based formulas of Newmark and Hall (1982).

$$R_A(B_{eff}) = \frac{2.12}{3.21 - 0.68 \log(B_{eff})} \quad (3.14)$$

$$R_V(B_{eff}) = \frac{1.65}{2.31 - 0.41 \log(B_{eff})} \quad (3.15)$$

where;

B_{eff} is the effective damping given by the expression:

$$B_{eff} = B_e + B_h \quad (3.16)$$

where;

B_e is the elastic damping and B_h is the hysteretic damping, which is a function of the yield and ultimate capacity points (ATC, 1996) as follows:

$$B_h = 63.7\kappa \left(\frac{A_{yi}}{A_u} - \frac{D_{yi}}{D_u} \right) \quad (3.17)$$

where;

κ is a degradation factor that defines the effective amount of hysteretic damping as a function of earthquake duration and energy-absorption capacity of the structure during cyclic earthquake load, as shown in Table 3.6, and A_{yi} and D_{yi} are obtained through an iterative process as a part of the capacity curve bilinearization.

Table 3.6 Degradation factor (κ) for Pre-code design, HAZUS (1999)

Building type		Pre-code design		
No	Label	Short	Moderate	Long
1	W1	0.50	0.30	0.10
2	W2	0.40	0.20	0.00
3	S1L	0.40	0.20	0.00
4	S1M	0.40	0.20	0.00
5	S1H	0.40	0.20	0.00
6	S2L	0.40	0.20	0.00
7	S2M	0.40	0.20	0.00
8	S2H	0.40	0.20	0.00
9	S3	0.40	0.20	0.00
10	S4L	0.40	0.20	0.00
11	S4M	0.40	0.20	0.00
12	S4H	0.40	0.20	0.00
13	S5L	0.40	0.20	0.00
14	S5M	0.40	0.20	0.00
15	S5H	0.40	0.20	0.00
16	C1L	0.40	0.20	0.00
17	C1M	0.40	0.20	0.00
18	C1H	0.40	0.20	0.00
19	C2L	0.40	0.20	0.00
20	C2M	0.40	0.20	0.00
21	C2H	0.40	0.20	0.00
22	C3L	0.40	0.20	0.00

Table 3.6 Degradation factor (κ) for Pre-code design, HAZUS (1999), (continued)

Building type		Pre-code design		
No	Label	No	Label	No
23	C3M	0.40	0.20	0.00
24	C3H	0.40	0.20	0.00
25	PC1	0.40	0.20	0.00
26	PC2L	0.40	0.20	0.00
27	PC2M	0.40	0.20	0.00
28	PC2H	0.40	0.20	0.00
29	RM1L	0.40	0.20	0.00
30	RM1M	0.40	0.20	0.00
31	RM2L	0.40	0.20	0.00
32	RM2M	0.40	0.20	0.00
33	RM2H	0.40	0.20	0.00
34	URML	0.40	0.20	0.00
35	URMM	0.40	0.20	0.00
36	MH	0.60	0.30	0.10
37	S3C3	0.40	0.20	0.00
38	W1C3	0.45	0.25	0.05
39	W2C3	0.40	0.20	0.00

Following the recommendations of Newmark and Hall (1982), B_e is elastic (pre-yield) damping of the model building type, which is:

5% for mobile home (MH),

5% - 7% for steel building (S),

7% for concrete (C) and pre-cast concrete building (P),

7% - 10% for reinforced masonry building (RM),

10% for un-reinforced masonry (URM) and masonry building (M),

10% -15% for wood building (W)

The methodology recognizes the importance of the duration of ground shaking on building response by reducing the effective damping (i.e., κ -factors) as a function of shaking duration. Dependent on the magnitude of the scenario earthquake, the effective damping is based on the assumption of different ground shaking durations:

- Magnitude, $M \leq 5.5$ short duration
- Magnitude, $5.5 \leq M \leq 7.5$ moderate duration
- Magnitude, $M \geq 7.5$ long duration

The new demand spectral acceleration $Sa(T)$ in units of gravity(g) is defined at short periods (acceleration domain), long period (velocity domain), and very long periods (displacement domain) using 5% damped response spectrum and dividing by the before mentioned factors following the expressions:

$$Sa(T) = \frac{Sa_{ASi} \left(0.4 + \frac{T}{T_A}\right)}{R_A(B_{eff})} \quad \text{for } 0 < T < T_A \quad (3.18)$$

$$Sa(T) = \frac{Sa_{ASi}}{R_A(B_{eff})} \quad \text{for } T_A < T < T_{AVB} \quad (3.19)$$

$$Sa(T) = \frac{\frac{Sa_{ALi}}{T}}{R_V(B_{eff})} \quad \text{for } T_{AVB} < T < T_{VD} \quad (3.20)$$

$$Sa(T) = \frac{\frac{Sa_{ALi} T_{VD}}{T^2}}{R_A(B_{eff})} \quad \text{for } T > T_{VD} \quad (3.21)$$

where;

S_{ASi} : 5% damped, short-period spectral acceleration for site class i, (g)

S_{ALi} : 5% damped, 1-second (long) period spectral acceleration

for site class i, (g)

- B_{TVD} : value of effective damping at the transition period T_{VD}
- T_{AVB} : transition period between acceleration and velocity domains as a function of the effective damping at this period which is defined by the equation:

$$T_{AVB} = T_{AVi} \frac{R_A(B_{TAVB})}{R_B(B_{TAVB})} \quad (3.22)$$

where;

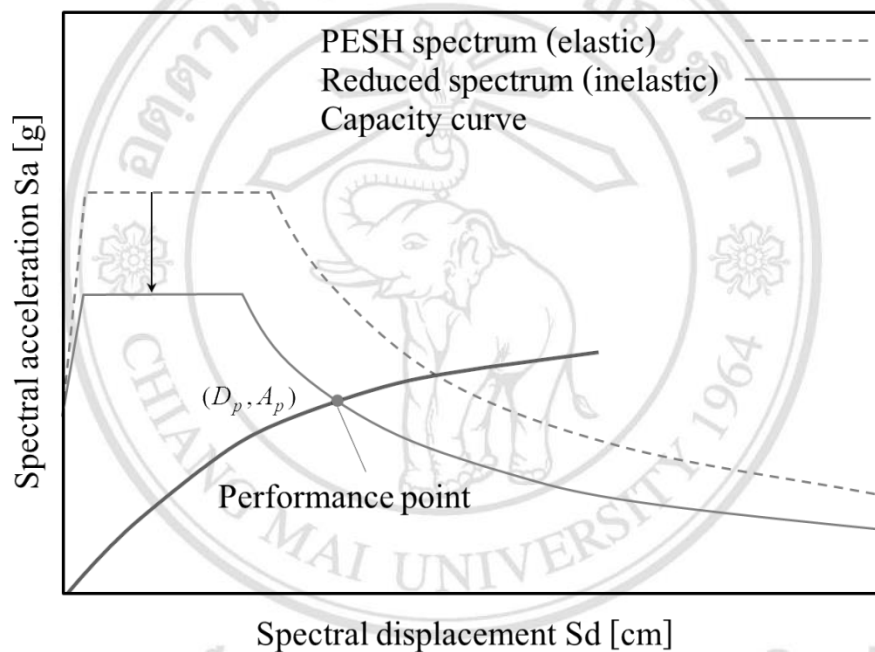
- T_{AVi} : transition period between 5%-damped constant spectral acceleration and 5%-damped constant spectral velocity for site class i
- B_{TAVB} : value of effective damping at the transition period T_{AVB}

The transition period T_{VD} is independent of effective damping and only depends on the moment magnitude. Therefore, the capacity-spectrum method procedure will be completed for each building assessed through execution of the following steps:

- (1) Calculation of the spectral accelerations and spectral displacements at the site in question taking into account soil response, so that response spectrum can be generated.
- (2) Creation or selection of a capacity curve for the respective building type reflecting the building's performance under an increasing, laterally applied (earthquake) load.
- (3) Determination of effective damping B_{eff} by specifying elastic damping B_e and by computing the hysteretic damping B_h . Based on this the calculation of both reduction factor R_A and R_V can be realized.
- (4) Reduction of the elastic response spectrum by reduction factor R_A and R_V to account for the increased damping that occurs at higher level of ground motion and consequently building response (non-linear behavior).
- (5) Superposition of the building capacity curve with the modified (inelastic) response spectrum (demand curve). The resulting building displacement is

estimated from the intersection of the building capacity curve and the response spectrum (performance point; see also Figure 3.11).

- (6) The estimated building displacement is later used to define the damage at the intercept of the fragility curve and damage probability curves (see Figure 3.12), displacements induced by an earthquake can be defined and the values used to compute the probability of damage in each of the four damage states (slight, moderate, extensive, and complete), as seen in Figure 3.13.



ลิขสิทธิ์มหาวิทยาลัยเชียงใหม่
Copyright © Chiang Mai University
All rights reserved

Figure 3.11 Capacity-spectrum curves

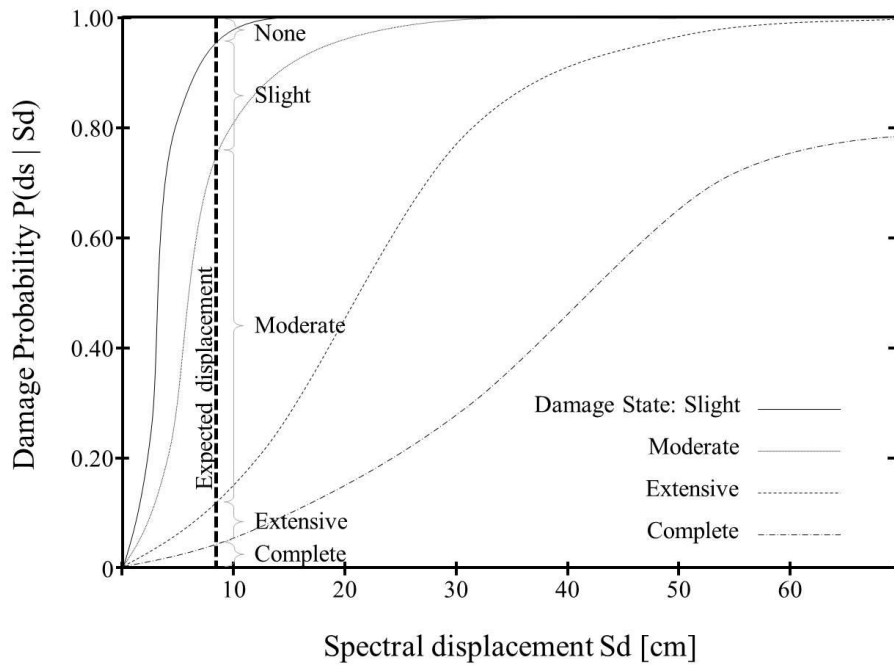


Figure 3.12 Cumulative damage probabilities

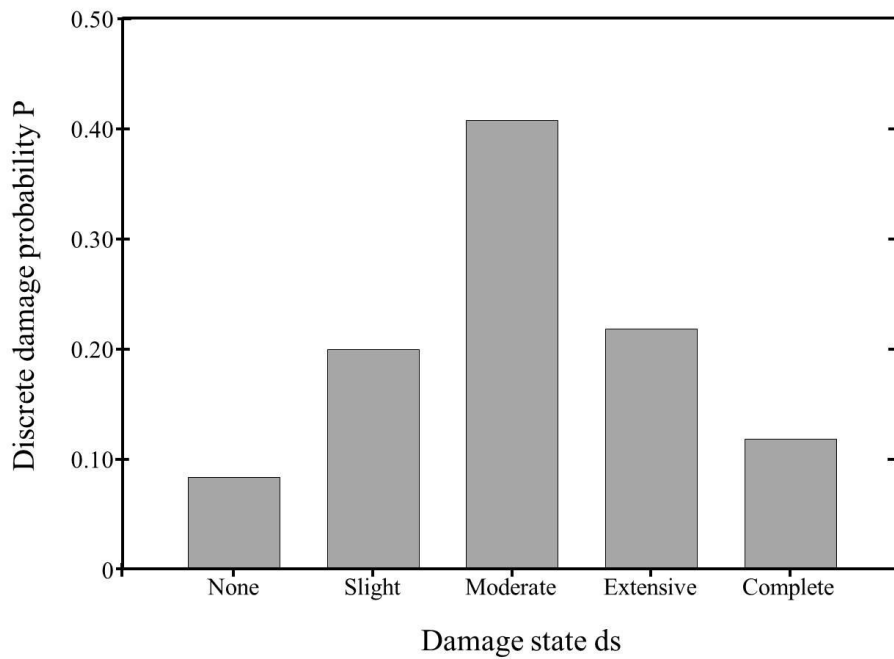


Figure 3.13 Discrete damage probabilities derived from the cumulative damage probabilities

3.5 Approximation of Number of Deaths

The loss model is only considering the direct human losses caused by structural damage not due to non-structural damage or follow-on hazards e.g. accidents from the road, fire that is followed by earthquake, heart disease. A more detailed description of severity levels is given in Table 3.7.

Table 3.7 Injury classification scale according to HAZUS

Injury level	Description
Severity 1	Injuries requiring basic medical aid that could be administered by paraprofessionals. These types of injuries would require bandages or observation. (Injuries of lesser severity which can be self-treated are not covered by HAZUS)
Severity 2	Injured requiring a greater degree of medical care and use of medical technology such as x-ray or surgery, but not expected to progress to a life threatening status.
Severity 3	Injuries that pose an immediate life threatening condition if not treated adequately and expeditiously.
Severity 4	Instantaneously killed or mortally injured.

In order to also cover extreme cases of occupancy which are strongly dependent on the time of the day (i.e., school occupancy only during daytime), the number of casualties will be computed for two different times of the day:

- (1) Nighttime scenario (call 02:00 AM): i.e., earthquake striking during nighttime.
- (2) Daytime scenario (call 02:00 PM): i.e., earthquake striking during daytime.

These scenarios are expected to generate the highest casualty numbers for the population at home (nighttime), the population at work/education (daytime), respectively.

3.5.1 Population distribution

The number of people in the study area was first estimated based on the building occupancy rate. The total population is classified into five different groups: (1) residential population, (2) commercial population, (3) education population, (4) industrial population, and (5) hotel population. The default value of population distributions is calculated for the two times of the day. Table 3.8 provides the relationships used to determine the population distribution.

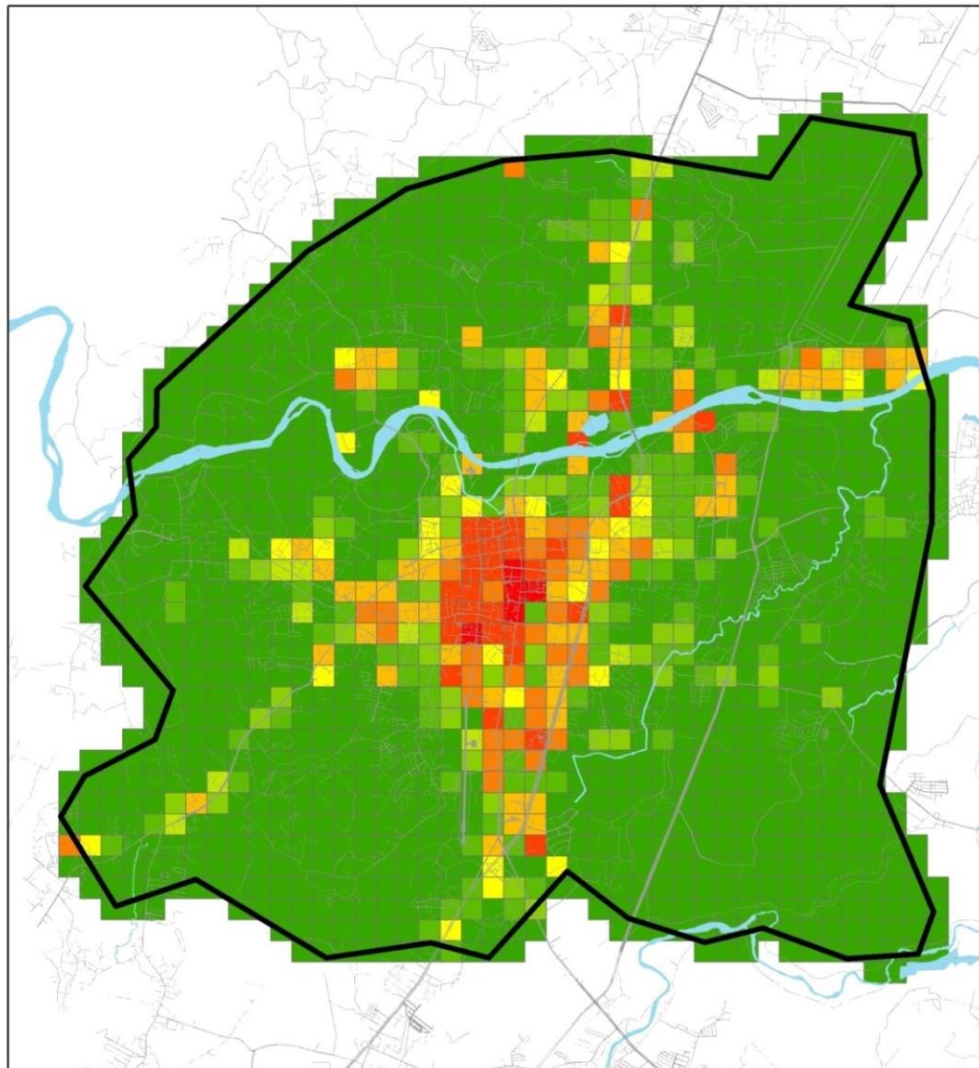
Table 3.8 Relationship to estimate the population distribution in the building

Distribution of people in census tract			
Occupancy	2:00 A.M.	2:00 P.M	5:00 P.M.
Indoors			
Residential	(0.999)0.99 (NRES)	(0.70)0.75(DRES)	(0.70)0.5(NDRES)
Commercial	(0.999)0.02 (COMW)	(0.99)0.98(COMW)+(0.80)0.20(DRES)+0.80(HOTEL)+0.80VISIT	0.98[0.50(COMW+0.10(NDRES))+0.70(HOTEL)]
Education		(0.90)0.80(GRADE)+0.80(COLLEGE)	(0.80)0.50(COLLEGE)
Industrial	(0.999)0.10 (INDW)	(0.90)0.80(INDW)	(0.90)0.50(INDW)
Hotels	0.999 (HOTEL)	0.19(HOTEL)	0.299(HOTEL)
Outdoors			
Residential	(0.001)0.99(NRES)	(0.3)0.75(DRES)	(0.3)0.5(DRES)
Commercial	(0.001)0.02(COMW)	(0.01)0.98(COMW)+(0.20)0.20(DRES)+(0.2)VISIT+0.50(1-PRFIL)0.05(POP)	0.02[0.50(COMW)+0.10(NRES)+0.70(HOTEL)+0.50(1-PRFIL)][0.05(POP)+1.0(COMM)]
Education		(0.01)0.80(GRADE)+0.20(COLLEGE)	(0.20)0.50(COLLEGE)
Industrial	(0.001)0.01(INDW)	(0.10)0.80(INDW)	(0.10)0.50(INDW)
Hotels	0.001(HOTEL)	0.01(HOTEL)	0.001(HOTEL)
Commuting			
	0.005(POP)	(PRFIL)0.05(POP)	(PRFIL)[0.05(POP)+1.0(COMM)]
		0.50(1-PRFIL)0.05(POP)	0.50(1-PRFIL)[0.05(POP)+1.0(COMM)]

where;

POP	is	Population in the area
DRES	is	Daytime residential population
NRES	is	Nighttime residential population
COMM	is	The number of people commuting
COMW	is	The number of people employed in the commercial sector
INDW	is	The number of people employed in the industrial sector
GRADE	is	Population, or students in grade school
COLLEGE	is	Population, or students who are on college and university
HOTEL	is	The number of people staying in hotels
PRFIL	is	A factor representing the proportion of commuters using automobiles, inferred from profile of the community (0.60 for dense urban area, 0.80 for less dense urban or suburban areas and 0.85 for rural)
VISIT	is	The number of regional residents who do not living in the study area. Default is set to zero.

The distribution of the population in Chiang Rai Municipality for daytime and nighttime are shown in Figures 3.14 and 3.15, respectively.



0 .5 1 2



Kilometers



Figure 3.14 Population distributions in Chiang Rai Municipality, daytime 2:00 PM

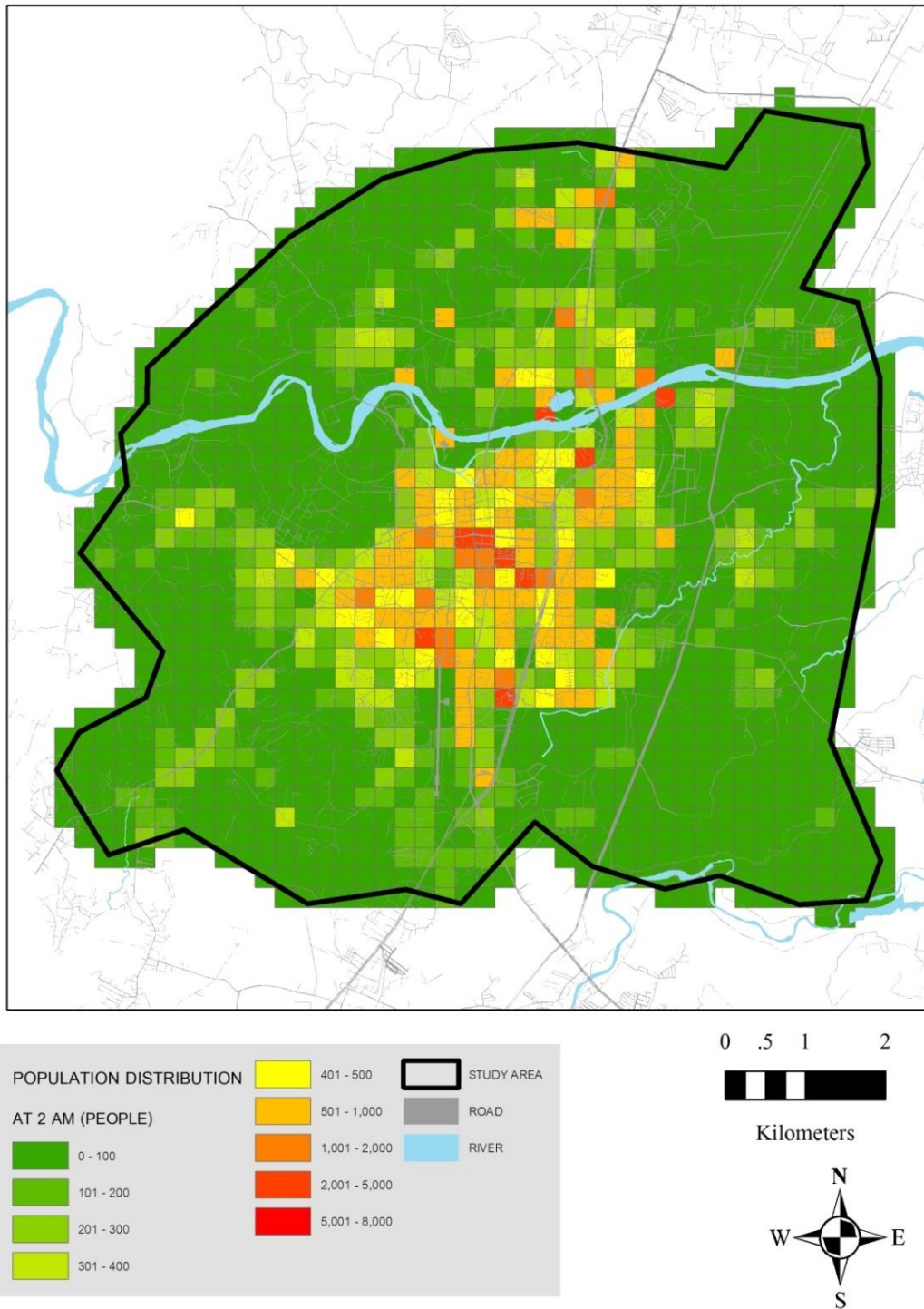


Figure 3.15 Population distributions in Chiang Rai Municipality, nighttime 2:00 AM

3.5.2 Human losses

To calculation of the injury or death is referred to the building damage level from the previous section: i.e., slight damage, moderate, extensive and complete or collapse.

The number of casualties is due to direct structural damage for any structure type. The estimates are based on the rate of injuries and loss of life that occurred as follows.

- (1) The rate of casualty severity level of the structure damaged in a slightly, moderate and extensive level.
- (2) The rate of casualty severity level of the structure damaged in a complete level without collapse.
- (3) The rate of casualty severity level of the structure damaged in a complete level with collapse.
- (4) Probability of collapse given a complete damage state.

Therefore, the rate of casualty severity level can be shown in Appendix B. Table 3.9 shows the percentage of buildings that collapsed.

Table 3.9 Percentage of building collapsed in complete level for each structural type

No.	Building Type	Probability of collapse given a complete damage state
1	W1	3.00%
2	W2	3.00%
3	S1L	8.00%
4	S1M	5.00%
5	S1H	3.00%
6	S2L	8.00%
7	S2M	5.00%
8	S2H	3.00%
9	S3	3.00%
10	S4L	8.00%
11	S4M	5.00%
12	S4H	3.00%
13	S5L	8.00%
14	S5M	5.00%
15	S5H	3.00%
16	C1L	13.00%
17	C1M	10.00%
18	C1H	5.00%
19	C2L	13.00%
20	C2M	10.00%
21	C2H	5.00%
22	C3L	15.00%
23	C3M	13.00%

Table 3.9 Percentage of building collapsed in complete level for each structural type
(continued)

No.	Building Type	Probability of collapse given a complete damage state
24	C3H	10.00%
25	PC1	15.00%
26	PC2L	15.00%
27	PC2M	13.00%
28	PC2H	10.00%
29	RM1L	13.00%
30	RM1M	10.00%
31	RM2L	13.00%
32	RM2M	10.00%
33	RM2H	5.00%
34	URML	15.00%
35	URMM	15.00%
36	MH	3.00%
37	S3C3	9.00%
38	W1C3	9.00%
39	W2C3	9.00%

The calculation of the number of human casualties basically follows the HAZUS approach (FEMA, 2001) as shown in Figure 3.16. The number of casualties due to direct structural damage for any given structure type, which does not consist of non-structural damage, level of building damage, and injury severity can be calculated by equations (3.23 – 3.27). However, the loss model applied here considered the level of severity as instantaneously killed or mortally injured.

$$P_{killed} = P_A \times P_E + P_B \times P_F + P_C \times P_G + P_D \times (P_H \times P_J + P_I \times P_K) \quad (3.23)$$

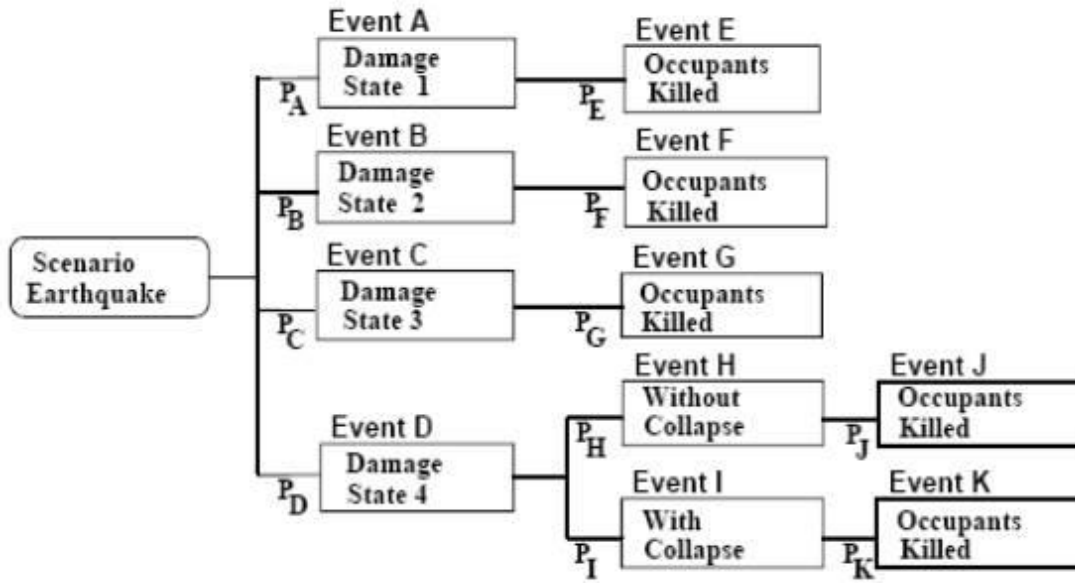


Figure 3.16 Casualty event tree model (Saadat *et al*, 2014)

$$P_{killed} = P_{killed (collapse)} + P_{killed (no-collapse)} \quad (3.24)$$

Where;

$$P_{killed (collapse)} = P_D \times P_I \times P_K \quad (3.25)$$

$$P_{killed (no-collapse)} = P_A \times P_E + P_B \times P_F + P_C \times P_G + P_D \times P_H \times P_J \quad (3.26)$$

Then;

$$EN_{Occupants\ killed} = N_{occupants} \times P_{killed} \quad (3.27)$$

Due to the different activities during one day, the numbers of casualties were computed for two different times e.g. nighttime (at 2:00 AM), and daytime (at 2:00 PM), respectively. At the nighttime, people usually stay at home. However, during the daytime, people are assumed to be working outside and are more likely to be in densely packed public and assembly buildings.

3.6 Re-estimation of losses after structural upgrading

The same methodology for estimating buildings damaged and numbers of casualties mentioned above were re-applied after the rehabilitation of a selected number of existing structures to improve their seismic performance. The buildings of higher importance such as hospital/emergency services, schools and government offices were selected for rehabilitation. The performance of the rehabilitated buildings was required to conform with regulations for moderate-seismicity, as shown in Tables 3.10 – 3.11, the capacity curve and degradation factor for each building type were used in earthquake damage re-estimate. Figure 3.17 shows the performance comparisons between those of the existing and upgraded buildings.

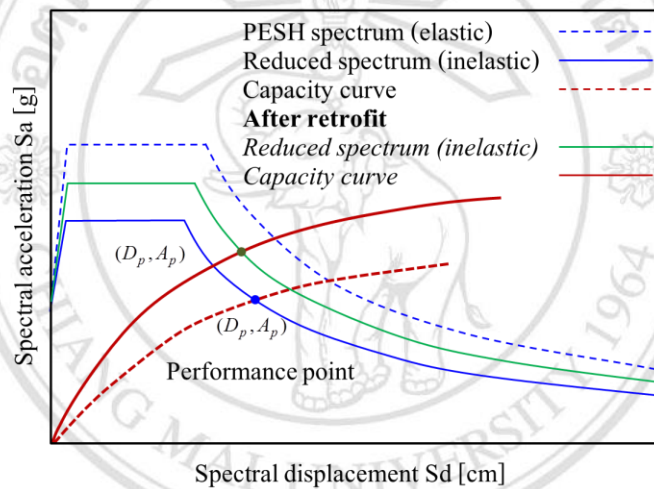


Figure 3.17 Capacity-spectrum curves after rehabilitation

Table 3.10 Capacity Curve for Moderate-Code Seismic Design Level

Building Type	Yield Capacity Point		Ultimate Capacity Point	
	D_y (cm.)	A_y (g)	D_u (in.)	A_u (g)
W1	0.360	0.300	6.480	0.900
W2	0.310	0.200	4.700	0.500
S1L	0.310	0.125	5.500	0.375
S1M	0.890	0.078	10.650	0.234
S1H	2.330	0.049	20.960	0.147
S2L	0.310	0.200	3.760	0.400
S2M	1.210	0.167	9.700	0.333
S2H	3.870	0.127	23.240	0.254

Table 3.10 Capacity Curve for Moderate-Code Seismic Design Level (continued)

Building Type	Yield Capacity Point		Ultimate Capacity Point	
	<i>D_y</i> (cm.)	<i>A_y</i> (g)	<i>D_u</i> (in.)	<i>A_u</i> (g)
S3	0.310	0.200	3.760	0.400
S4L	0.190	0.160	2.590	0.360
S4M	0.550	0.133	4.910	0.300
S4H	1.740	0.102	11.760	0.228
C1L	0.200	0.125	3.520	0.375
C1M	0.580	0.104	6.910	0.312
C1H	1.010	0.049	9.050	0.147
C2L	0.240	0.200	3.600	0.500
C2M	0.520	0.167	5.190	0.417
C2H	1.470	0.127	11.020	0.317
C3L	0.240	0.200	2.700	0.450
PC1	0.360	0.300	4.320	0.600
PC2L	0.240	0.200	2.880	0.400
PC2M	0.520	0.167	4.150	0.333
PC2H	1.470	0.127	8.820	0.254
RM1L	0.320	0.267	3.840	0.533
RM1M	0.690	0.222	5.540	0.444
RM2L	0.320	0.267	3.840	0.533
RM2M	0.690	0.222	5.540	0.444
RM2H	1.960	0.169	11.760	0.338
URML	0.360	0.300	3.600	0.600
MH	0.180	0.150	2.160	0.300
S3C3	0.275	0.200	3.230	0.425
W1C3	0.300	0.250	4.590	0.675
W2C3	0.275	0.200	3.700	0.475

All rights reserved

Table 3.11 Degradation factor (κ) for Moderate-code design (HAZUS, 1999)

Building type		Moderate-code design		
No	Label	Short	Moderate	Long
1	W1	0.90	0.60	0.30
2	W2	0.80	0.40	0.20
3	S1L	0.80	0.40	0.20
4	S1M	0.80	0.40	0.20
5	S1H	0.80	0.40	0.20
6	S2L	0.60	0.40	0.20
7	S2M	0.60	0.40	0.20
8	S2H	0.60	0.40	0.20
9	S3	0.60	0.40	0.20
10	S4L	0.60	0.40	0.20
11	S4M	0.60	0.40	0.20
12	S4H	0.60	0.40	0.20
13	S5L	0.50	0.30	0.10
14	S5M	0.50	0.30	0.10
15	S5H	0.50	0.30	0.10
16	C1L	0.80	0.40	0.20
17	C1M	0.80	0.40	0.20
18	C1H	0.80	0.40	0.20
19	C2L	0.80	0.40	0.20
20	C2M	0.80	0.40	0.20
21	C2H	0.80	0.40	0.20
22	C3L	0.50	0.30	0.10
23	C3M	0.50	0.30	0.10
24	C3H	0.50	0.30	0.10
25	PC1	0.60	0.40	0.20
26	PC2L	0.60	0.40	0.20
27	PC2M	0.60	0.40	0.20
28	PC2H	0.60	0.40	0.20
29	RM1L	0.80	0.40	0.20
30	RM1M	0.80	0.40	0.20
31	RM2L	0.80	0.40	0.20
32	RM2M	0.80	0.40	0.20
33	RM2H	0.80	0.40	0.20
34	URML	0.50	0.30	0.10
35	URMM	0.50	0.30	0.10
36	MH	0.80	0.40	0.20
37	S3C3	0.55	0.35	0.15
38	W1C3	0.70	0.45	0.20
39	W2C3	0.65	0.35	0.15

3.7 Fuzzy Application in Risk Model

Earthquake risk assessment is the determination of risk related to the earthquake consequence. Variations include seismic building vulnerability, seismic hazard and building importance. However, the parameters are uncertain in nature and difficult to measure. In this complicated evaluation, sophisticated risk assessments are often made. Ellingwood (2001) reviewed earthquake risk assessment of building structures pertaining to probability-based method. In his work, the inherent randomness and modeling uncertainty in forecasting building performance were quantitatively examined. Qualitatively, fuzzy logic has been widely adopted for the vague information. Deb and Kumar (2004) qualitatively conducted assessment of seismic damage in reinforced concrete buildings by applying the de-fuzzification method. The fuzzy linguistic variable was inverted to damage index that correspond to the damage state. The damage index was defined from 0 to 1 indicating damage level from nonstructural damage (no building damage) to building collapse, respectively.

Sen (2010) proposed the fuzzy logic method for building earthquakes assessment satisfying multiple performance objectives including both quantitative and qualitative information sets. For exterior rapid inspection, building resistance against earthquake assessment was performed by considering several of the measured and calculated factors such as the storey number, cantilever extension, soft storey, weak storey, building quality, pounding effect, hill-slope effect, and peak ground velocity. Rapid interior inspection was performed by Sen (2011) considering building height, story height ratio, cantilever extension ratio, moment of inertia, column and shear wall area percentages, and the number of frames and area of influence. Haoxiang *et al.* (2013) showed the applicability of fuzzy set methodology to seismic damage assessment in reinforced concrete structures. Kamran *et al.* (2014) proposed fuzzy multi-criteria decision making (MCDM) with an aggregated fuzzy seismic risk index (FSRi) which has potential for mitigate the exposure of cities in Iran to access seismic risk. The result helps decision makers to screen and prioritize multiple regions in seismically prone areas.

From the above literature review, past researches in the field of seismic risk assessment have been done mainly for building damage. However, the seismic risk assessment is not limited to building vulnerability but it also covers other viewpoints.

Figure 3.18 shows venn diagram illustrating the risk factors other than the building vulnerability including the site seismic hazard and importance of building (building occupancy type). The overlapping area or intersection of the factors then represents the set of all seismic risk. Hence, the risk mitigation is made on the overlapped area.

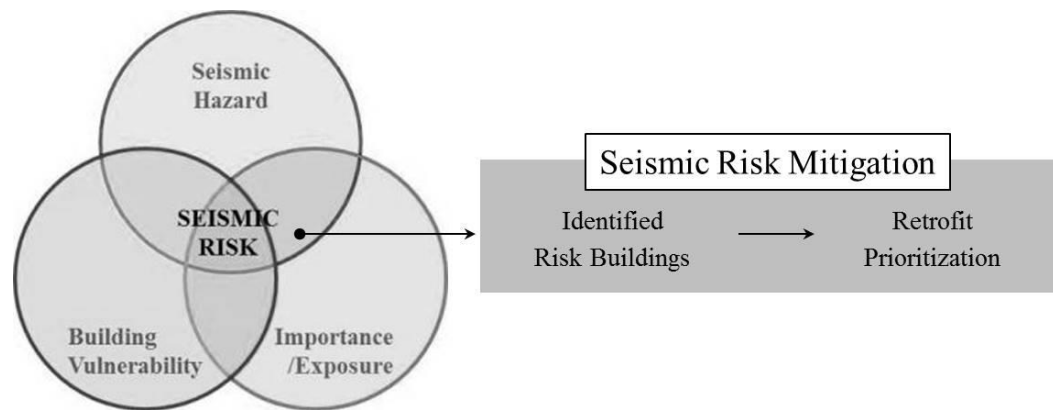


Figure 3.18 Venn diagram for earthquake risk assessment
(Modified from Tesfamariam and Saatcioglu, 2008)

3.7.1 Risk Assessment Model

In this study, seismic risk assessment approach is proposed for prioritizing building to incremental retrofit in Chiang Rai municipality area, located in the northern region of Thailand. First, risk factors were identified comprising of (1) Building vulnerability, (2) Seismic Hazard and (3) Building importance. The complex problem of risk assessment can be drawn up in the hierarchical structure, as shown in Figure 3.18. From the figure, Level 1 of the hierarchy is seismic risk or the total risk of the analysis. The total seismic risk score was computed by integrating the parameters at Level 2 that reflects building damageability and building importance/exposure. At Level 3, the building importance/exposure parameter was computed by building occupancy and/or historic value.

The building damageability was calculated by integrating the parameters at Level 3 composing of site seismic hazard and building vulnerability. The site seismic hazard was determined by peak ground acceleration from the assumed earthquake. Magnitude and location of the epicenter were determined based on seismic hazard map, location of

seismic fault and past earthquake records. The assumed epicenter was the location where the earthquake had occurred once and on the fault line. The building vulnerability factors were obtained from field survey of all building using Rapid Visual Screening method described in FEMA 154 (2002a). The method evaluated seismic performance of buildings based on (i) building type, (ii) vertical irregularity, (iii) plan irregularity, (iv) number of story, (v) year of building construction and (vi) soil type.

For the building importance defined by different types of occupancy, Analytical Hierarchy Process (AHP) was adopted for the evaluation. The factors contained qualitative evaluation and hence need to be converted into fuzzy logic model. Using the three risk factors, the total risk index was calculated through logical reasoning, integrating all the factors as shown in Figure 3.19. This logical reasoning was interpreted in the IF – THEN rule based form or deductive form in the inference, which is consistent with the logic of human thought. Finally, the total risk of all buildings in the study area was obtained and retrofit prioritization was identified accordingly.

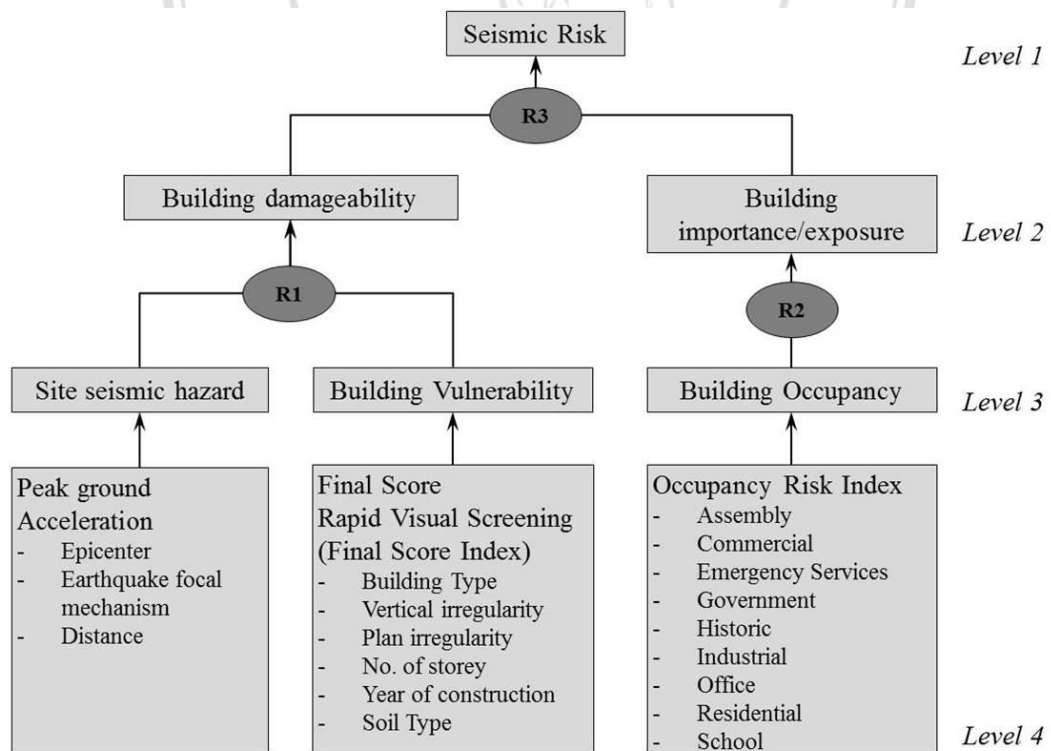


Figure 3.19 Hierarchical building risk assessments from earthquake hazard

3.7.2 Fuzzy logic Modeling

Zadeh (1965) introduced the application of fuzzy logic and fuzzy set theory to risk management. Fuzzy logic provides a language with semantics to translate qualitative knowledge into numerical reasoning, which enables modeling complex systems like buildings risk assessment. The strength of fuzzy logic is that it can integrate descriptive (linguistic) knowledge and numerical data to fuzzy model and use approximate reasoning algorithms to propagate the uncertainties throughout the decision process. With building damage level, building important and building vulnerability, Fuzzy logic model was hence adopted here taking possibility of incidence and the severity of the risk to be accounted. A fuzzy set describes the relationship between an uncertain quantity x in set and membership function μ_x , which ranges between 0 and 1.

The membership function is a critical important input for the fuzzy logic system. It requires translating the qualitative description into a quantitative measure. Several geometric mapping functions have been widely adopted, such as triangular, trapezoidal and S-shaped membership functions, it is difficult for an expert to use an exact numerical value to represent his/her degree of preference. However, triangular and trapezoidal MFs are the most frequently used in seismic risk assessment practice. They are good enough to capture the vagueness of these linguistic assessments with a fuzzy modeling mechanism for quantifying seismic hazard, building vulnerability and building occupancy.

The fuzzy inference system (FIS) contains three basic steps, as described by Zadeh, 1973. First, fuzzification linguistic variables are transformed into numerical variables with an assumed scale. This step is normally called fuzzification. Second, variables inference relationships between the variables are integrated using IF-THEN rules. The inference mechanism using approximate reasoning algorithms are adopted to formulate relationships. Third, defuzzification is the process of producing a quantifiable resulting in crisp number.

The general scheme of fuzzy logic based decision making system is shown in Figure 3.20. From the figure, the linguistic transformations of the earthquake intensity

are classified into three ranges as “Low or L”, “Medium or M” and “High or H”. With the use of the triangular membership function, the maximum membership varies linearly to the minimum value. The “Low” earthquake intensity is defined as PGA between 0.0g-0.5g. with the membership value from 1 to 0. For the “Medium” earthquake intensity, the PGA is in the range of 0.0g-1.0g with the membership value equal to 1 and the PGA of 0.5g. The PGA between 0.5g-1.0g is defined for “High” earthquake intensity with the membership from 0-1.0. The same transformation procedure was adopted for the building vulnerability and building importance risk factors.

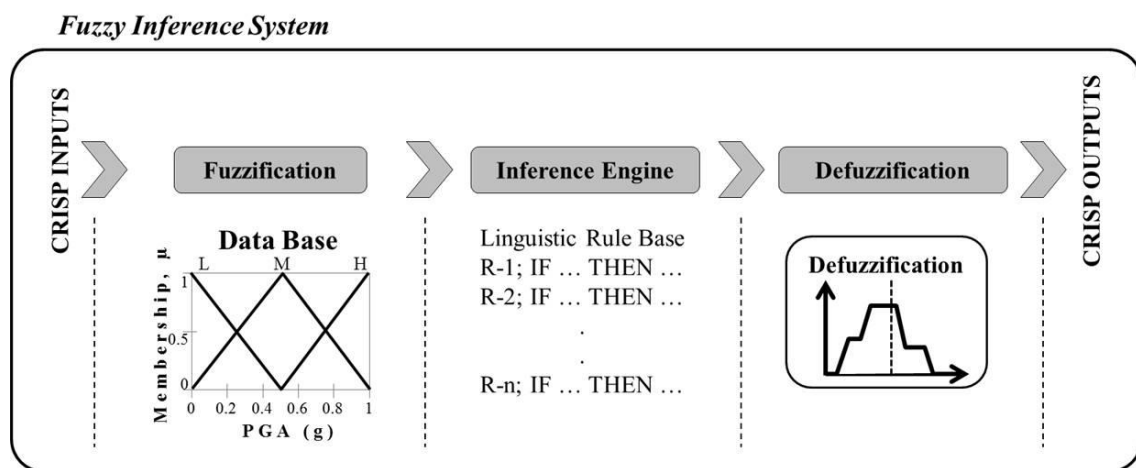


Figure 3.20 Fuzzy inference system for risk assessment

3.8 Application of Artificial Neural Network for Risk Assessment

Previously, the methods for identification of building risk with high potential to damage and building important are mainly based on capacity-spectrum method and qualitative assessment. Thus, it consumes times to overall analysis. This section presents an artificial neural network approach for identification of building risk on regional seismic hazard zone. It is a new research method for building risk assessment modeling with qualitative and quantitative data. To demonstrate the framework, a prototype is developed and tested on Chiang Rai Municipality. The results are compared against the previous sections in the study which total risk index of building. The results show a correlation between the output of the proposed method and existing

method. The results confirms that this method is not only a cheaper one but also time saving, especially when data are uncertain and incomplete. Furthermore, research methodology helps decision makers to determine which hazard building is the most important ones, and ultimately to decide which hazard mitigation strategies should be employed.

That system is trained by a learning algorithm from artificial neural network theory. This approach employs heuristic learning strategies derived from the domain of neural networks theory to support the development of a total risk assessment. Although fuzzy logic can encode expert knowledge using linguistic label, it usually takes a lot of time to turn the membership functions which quantitatively define these linguistic labels. Moreover, applications of fuzzy systems are restricted to the fields where expert knowledge is available and the number of input variables is small. Neural network learning techniques can automate this process and reduce development time and cost while improving performance and extracting fuzzy rules from numerical data automatically (Effati and others, 2014). Figure 3.21 shows the artificial neural network structure which is proposed for identification of total risk index of building.

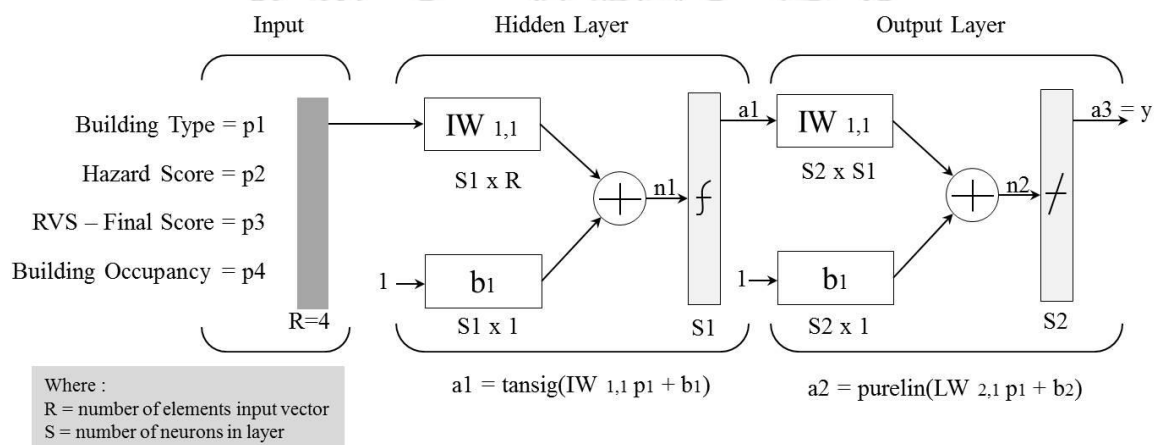


Figure 3.21 Proposed neuro structure of total risk index of building

Training process of this neural is carry out in two step, forward and backward. In the forward pass of the learning algorithm, processing proceeds up to hidden layer. In hidden layer the consequence parameters are adjusted and the network output indicates a certain risk level. In the backward pass, the error rates propagat backward and the

premise parameters in layer 1 are updated. In fact, for the parameters in the layer1, back propagation algorithm is used. For training the parameters in the hidden layer, a variable of least-squares approximation or back-propagation algorithm is used. Therefore, this system uses a neural learning algorithm in order to train the network.



ลิขสิทธิ์มหาวิทยาลัยเชียงใหม่
Copyright© by Chiang Mai University
All rights reserved